



Comparison between braking and steering yaw moment controllers considering ABS control aspects

Jeonghoon Song^{a,*}, Woo Seong Che^b

^a Department of Mechatronics Engineering, Tongmyong University, Yongdang-Dong, Nam-Gu, Busan 608-711, Republic of Korea

^b Department of Electrical and Mechatronic Engineering, Kyungsung University, Daeyeon-Dong, Nam-Gu, Busan 608-736, Republic of Korea

ARTICLE INFO

Keywords:

BYMC (braking yaw moment controller)
SYMC (steering yaw moment controller)
ABS (anti-lock braking system)
Vehicle stability control

ABSTRACT

Two yaw motion control systems that improve a vehicle lateral stability are proposed in this study: a braking yaw motion controller (BYMC) and a steering yaw motion controller (SYMC). A BYMC controls the braking pressure of the rear inner wheel, while a SYMC steers the rear wheels to allow the yaw rate to track the reference yaw rate. A 15 degree-of-freedom vehicle model, simplified steering system model, and driver model are used to evaluate the proposed BYMC and SYMC. A robust anti-lock braking system (ABS) controller is also designed and developed. The performance of the BYMC and SYMC are evaluated under various road conditions and driving inputs. They reduce the slip angle when braking and steering inputs are applied simultaneously, thereby increasing the controllability and stability of the vehicle on slippery roads. The SYMC performs better than the BYMC because the SYMC vehicle has four-wheel steering. However, both the BYMC and SYMC vehicles show improved performance during lane-change maneuvers.

Crown Copyright © 2008 Published by Elsevier Ltd. All rights reserved.

1. Introduction

Recently, vehicle stability control systems, which maintain vehicle stability to provide an active safety system, have become popular in the automotive market. These systems detect or estimate sideslip information when the vehicle has a yawing attitude, and then manage the yaw moment by actively controlling the braking force of the rear inner wheel or steering angle of the rear wheels independently of the driver. Several types of vehicle yaw moment controllers (YMC, also known as ESP (electronic stability program) or VDC (vehicle dynamics control)) have been proposed and developed. Among them, the braking yaw moment controller (BYMC), which controls the brake pressure, is the most famous and widely studied because it does not require any complicated hardware if the vehicle is equipped with an anti-lock braking system (ABS). BYMC controllers consist of an ABS and YMC, and use a yaw rate feedback method that uses the desired yaw rate as the reference value [1–3].

However, recent research and development has shown that four-wheel steering systems can effectively improve the handling behavior of vehicles. These handling improvements provide better maneuverability at low speeds and reduce the delay in path tracking by setting the rear wheel steering angle in the direction oppo-

site to the front wheel steering angle. At high speeds, four-wheel steering systems improve vehicle stability by turning all the wheel steering angles in the same direction, leading to greater passenger relaxation [4,5].

This study proposes a new vehicle stability control method that uses the yaw rate feedback method found in a BYMC. However, to achieve lateral stability, the proposed system is a steering yaw motion controller (SYMC), which controls the steering angle of the rear wheels. Thus the SYMC system is a four-wheel steering system. It consists of an ABS to maintain longitudinal stability and an SYMC to enhance lateral stability. The most important objective of this study is to develop vehicle stability control systems and compare their performance. Siahkalroudi and Naraghi [6] proposed a dual-steering scheme that controls both the rear and front steering angles to improve vehicle stability. However, controlling the front steering angle will reduce the overall controllability, and their results may be difficult to implement on a real vehicle. Fennel and Ding [1] and Van Zanten [2] described the electronic stability program (ESP) of Bosch and Continental TEVES, respectively. However, those systems only use a braking control scheme.

In this study, a 15 degree-of-freedom vehicle model, simplified electric power steering system (EPS) model, and driver model are used to create a BYMC and the proposed SYMC. The developed BYMC and SYMC are constructed using these numerical models, a sliding mode nonlinear ABS controller and a PID mode YMC controller.

* Corresponding author. Tel.: +82 51 629 1537; fax: +82 51 629 1529.
E-mail address: jhsong@tu.ac.kr (J. Song).

Nomenclature

A_w	area of master cylinder	R_b	distance from center of wheel to brake path
a	distance from cg to the front wheel	R_w	wheel radius
b	distance from cg to the rear wheel	T_{assist}	assist torque at pinion
B_{roll}	roll axis torsional damping	T_b	brake torque
F_D	drag force	T_{load}	load torque at pinion
F_{fric}	friction force acting in the wheel plane	T_{roll}	wheel torque due to resistance
F_n	normal force	t_f, t_r	front and rear wheel distance
F_x	longitudinal force	u_{EPS}	motor input voltage
F_y	lateral force	β	side slip angle
h_s	distance from sprung mass cg to roll axis	δ	steering angle at the wheel
I_{roll}	vehicle moment of inertia around roll axis	γ	yaw angle
I_w	rotating inertia of a wheel	φ	roll angle
I_z	vehicle moment of inertia around z axis	λ_d	desired slip
K_a	torque constant of power assist steering system	λ_s	wheel slip
K_E	back emf constant	μ	friction coefficient
K_{roll}	roll axis torsional stiffness	θ_p	rotational degree of pinion
M_z	tyre aligning moment	θ_{sw}	steering degree input at steering wheel
M_{zw}	aerodynamics yaw moment	θ_w	rotational degree of wheel
N_i	gear ratio of power assist steering system	τ_s	time delay of driver's response
P_b	brake fluid pressure	Γ	torque
R_a	armature resistance		

2. Vehicle model and ABS controller**2.1. Vehicle model**

The author has previously developed a nonlinear 15 degree-of-freedom vehicle model (Fig. 1) [7] and a simplified electric power steering system model (Fig. 2) [8]. The vehicle model is constructed from many sub-models, such as the powertrain, suspension, tyres, chassis, road conditions, and so on, and the effect of each sub-system should be considered.

Fig. 1 defines the axis system and necessary degrees of freedom. The essential vehicle and tyre force variables that can handle a full range of maneuvering conditions from nominal to limiting performance conditions are also defined.

$$m_{total}(\dot{v}_x - v_y\dot{\gamma}) = \sum_{i=1}^4 FX_i - F_D \cos \beta \quad (1)$$

$$m_{total}(\dot{v}_y + v_x\dot{\gamma}) = \sum_{i=1}^4 FY_i - F_D \sin \beta \quad (2)$$

$$\Gamma = I_z \frac{d^2\gamma}{dt^2} = aFY_1 + \frac{t_f}{2}FX_1 + aFY_2 - \frac{t_f}{2}FX_2 - bFY_3 + \frac{t_r}{2}FX_3 - bFY_4 - \frac{t_r}{2}FX_4 + M_{zlf} + M_{zrf} + M_{zlr} + M_{zrr} + M_{zw} \quad (3)$$

$$I_{roll}\ddot{\varphi} + B_{roll}\dot{\varphi} + K_{roll}\varphi = m_sgh_s \sin \varphi - m_s(\dot{v}_y + v_x\dot{\gamma})h_s \cos \varphi \quad (4)$$

$$I_{wi}\ddot{\theta}_{wi} = -T_b - F_{xi}R_w - T_{rolli} = -P_{bi}A_wR_b - F_{xi}R_w - F_{rolli}R_w \quad (5)$$

where i in Eqs. (1)–(3) is 1, 2, 3 and 4, and represents the front left, front right, rear left, and rear right wheels, respectively. m_{total} is the total mass of the vehicle, which consists of the sprung mass (m_s), front unsprung mass (m_{uf}), and rear unsprung mass (m_{ur}) [5,8].

Eqs. (1) and (2) represent the vehicle dynamic to x and y direction and Eqs. (3) and (4) describe the vehicle yaw and roll movement, respectively. Eq. (5) expresses the wheel dynamics model. The forces generated at each wheel are calculated as

$$FX_i = F_{xi} \cos \delta_i - F_{yi} \sin \delta_i \quad (6)$$

$$FY_i = F_{yi} \sin \delta_i + F_{xi} \cos \delta_i \quad (7)$$

Table 1 represents the vehicle parameters.

2.1.1. Simplified electric power steering system model

From Fig. 2 and Newton's second law, the torques applied on the steering column and pinion of an electric power steering system can be calculated by [8]:

$$J_{eq}(\ddot{\theta}_p + B_{eq}(\dot{\theta}_p - \dot{\theta}_{sw}) + K_{eq}(\theta_p - \theta_{sw})) = T_{assist} + T_{load} \quad (8)$$

where J_{eq} is the total inertia, which includes the motor, gear train, pinion, rack, tie rod, and tyre referred to the pinion axis. B_{eq} is the effective damping coefficient referred to the pinion axis, and K_{eq} represents the stiffness of the steering column.

The assist torque can be represented as follows:

$$T_{assist} = \frac{N_1 K_a}{R_a} (u_{EPS} - K_E N_1 \dot{\theta}_p) \quad (9)$$

where K_a is the torque constant, which depends on the angle difference ($\theta_p - \theta_{sw}$) and vehicle velocity.

2.1.2. Rolling resistance force

The rolling resistance force at the tyre is defined as

$$F_{rolli} = f_r \times F_{ni} \quad (10)$$

where the rolling resistance coefficient, f_r , is [9,10]

$$f_r = f_0 + 3.24f_s(K_{mph}v_{xt}/100)^{0.25}$$

where $f_0 = 0.0105$ and $f_s = 0.0055$ are curve-fit parameter coefficients, and $K_{mph} = 2.237$ is a scaling constant that converts miles per hour (mph) to meters per second (m/s). v_{xt} is the speed of the wheel center in the direction that the tyre is heading, and is independent for each wheel.

2.1.3. Wheel slip calculation

The ABS controller modifies the brake pressure based on the slip. Slip is defined in terms of how close each wheel is to locking. The obtainable braking force depends on slip, which is defined as

$$\lambda_{si} = \frac{v_{xti} - \dot{\theta}_{wi}R_w}{v_{xti}} \quad (11)$$

where v_{xt} is the speed of the wheel center in the direction that the tyre is heading, and is independent for each wheel.

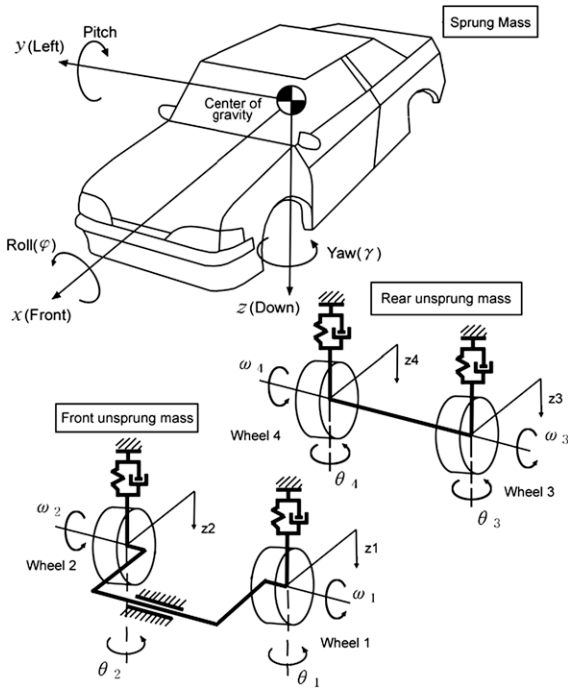


Fig. 1. Fifteen degrees of freedom vehicle model.

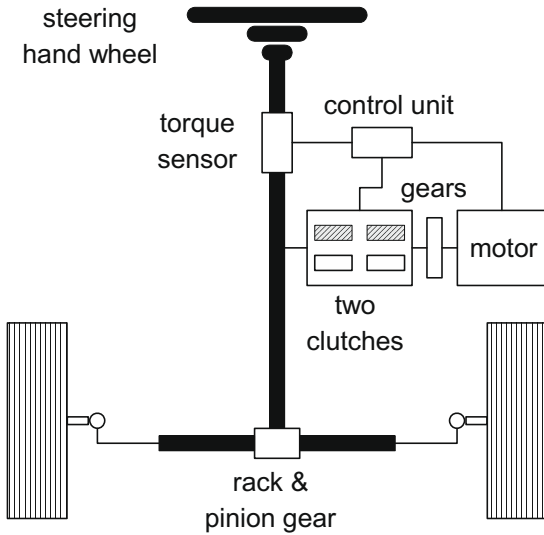


Fig. 2. Simplified steer system.

2.1.4. Friction coefficient calculation

The friction behavior of the wheels can be approximated using parametric characteristics. The friction, or cohesion coefficient, μ , is defined as

$$\mu = \frac{F_{fric}}{F_n} \quad (12)$$

The friction coefficient can be calculated using the method of Burckhardt [10,11].

$$\mu(\lambda_{Resi}) = c_1 [1 - \exp(-c_2 \lambda_{Resi})] - c_3 \lambda_{Resi} \quad (13)$$

where λ_{Res} is the geometrical sum of the slip and slip angle. The Burckhardt approach, Eq. (13) can be extended via a pair of factors, where c_4 describes the influence of a higher drive velocity and c_5 the influence of a higher wheel load. The resulting friction coefficient is then given by

$$\mu(\lambda_{Resi}) = \{c_1 [1 - \exp(-c_2 \lambda_{Resi})] - c_3 \lambda_{Resi}\} \times \exp(-c_4 \lambda_{Resi} v_{COG}) \times (1 - c_5 F_n^2) \quad (14)$$

where v_{COG} is the velocity of the center of gravity. Table 2 gives the parameters c_1 , c_2 , and c_3 for various road surfaces. Parameter c_4 ranges from 0.02 to 0.04 s/m and $c_5 = 0.00151 \text{ kN}^{-2}$.

2.2. Nonlinear sliding mode ABS controller

In general, the stopping distance decreases as the braking torque increases, unless the wheels slide [5,12]. Therefore, a controller that maintains a suitable braking torque is required to ensure that the stopping distance remains as short as possible. This is the main role of an ABS. The other important objective of an ABS is to maintain vehicle steerability while braking. Severe braking maneuvers will cause the wheels to lock, resulting in loss of control.

A sliding mode controller is introduced in this study. From Eq. (5), the wheel dynamics of a vehicle can be expressed by

$$\dot{\theta}_{wi} = -K_i u_i - \tau_{zi} - \tau_{ri} \quad (15)$$

Let $K_i = A_w R_b / I_{wi}$, $\tau_{zi} = F_{xi} R_w / I_{wi}$, $\tau_{ri} = F_{rolli} R_w / I_{wi}$, and the control input $u_i = P_{bi}$. The dynamics of τ_{zi} and τ_{ri} are not known exactly, but they can be estimated as $\hat{\tau}_{zi}$ and $\hat{\tau}_{ri}$. The estimation error for τ_{zi} and τ_{ri} is assumed to be bounded by known values of τ_{zi}^* and τ_{ri}^* . To ensure that the slip of the braking system, λ_{si} tracks the desired slip, λ_{di} , the sliding surface is defined as

$$S = \left(\frac{d}{dt} + \lambda \right)^{n-1} \int_0^t \lambda_r dr = \lambda_r + \lambda \int_0^t \lambda_r dr \quad (16)$$

where λ is a strictly positive constant, r is the variable of interest, $\lambda_r = \lambda_{di} - \lambda_{si}$, and $n = 2$. The derivative of the sliding surface is

$$\begin{aligned} \dot{S} &= \dot{\lambda}_r + \lambda \lambda_r = \frac{R_w}{\dot{\lambda}^2} (\ddot{\theta}_{wi} \dot{\lambda} - \dot{\theta}_{wi} \ddot{\lambda}) + \lambda (\lambda_{di} - \lambda_{si}) \\ &= \frac{R_w}{\dot{\lambda}^2} \left[-(K_i u_i + \tau_{zi} + \tau_{ri}) \dot{\lambda} - \dot{\theta}_{wi} \ddot{\lambda} + \frac{\dot{\lambda}^2}{R_w} (\lambda_{di} - \lambda_{si}) \right] \end{aligned} \quad (17)$$

where x is the vehicle displacement. The best approximation, \hat{u} , of a continuous control law that gives $\dot{S} = 0$ is

Table 2

Parameter sets for friction coefficient characteristics.

	c_1	c_2	c_3
Asphalt, dry	1.2801	23.99	0.52
Asphalt, wet	0.857	33.822	0.347
Concrete, dry	1.1973	25.168	0.5373
Snow	0.1946	94.129	0.0646
Ice	0.05	306.39	0

Table 1

Vehicle specifications.

m_{total}	1280 kg	t_f, t_r	1.33 m
m_s	1160 kg	N_i	12
m_{uf}	60 kg	A_w	0.0013 m ²
m_{ur}	60 kg	λ_d	0.2
I_{roll}	750 kgm ²	τ_s	0.1–0.3 s
I_w	2.1 kgm ²	J_{eq}	0.05 kgm ²
I_z	2500 kgm ²	B_{eq}	80 Nm/(rad/s)
K_{roll}	45000 Nm/rad	K_{eq}	30000 Nm/rad
B_{roll}	2600 Nm/(rad/s)	a_1	250
R_b	0.16 m	a_2	60
R_w	0.3 m	a_3	3
a	1.203 m	L	10 m
b	1.217 m	h_s	0.2 m

$$\hat{u}_i = -\frac{1}{\hat{x}K_i} \left[(\hat{\tau}_{zi} + \hat{\tau}_{ri})\dot{x} + \dot{\theta}_{wi}\ddot{x} - \frac{\dot{x}^2\lambda}{R_w}(\lambda_{di} - \lambda_{si}) \right] \quad (18)$$

if we define

$$\bar{u}_i = \frac{\tau_{ri}^* + \tau_{zi}^* + \eta}{K_i} \text{sgn}(S) \quad (19)$$

where η is a strictly positive constant. Since $u_i = \hat{u}_i + \bar{u}_i$, the control input u is as follows:

$$u_i = -\frac{1}{\hat{x}K_i} \left[(\hat{\tau}_{zi} + \hat{\tau}_{ri})\dot{x} + \dot{\theta}_{wi}\ddot{x} - \frac{\dot{x}^2\lambda}{R_w}(\lambda_{di} - \lambda_{si}) \right] + \frac{\tau_{ri}^* + \tau_{zi}^* + \eta}{K_i} \text{sgn}(S) \quad (20)$$

Eq. (20) satisfies the next sliding condition,

$$\frac{1}{2} \frac{d}{dt} S^2 = S \times \dot{S} \leq -\eta |S| \quad (\eta \geq 0) \quad (21)$$

The chattering problem caused by a control discontinuity in the $\text{sgn}(S)$ function can be eliminated by using a thin boundary layer with a thickness of Φ next to the switching surface.

3. Yaw motion controller

The main task of a YMC is to limit the slip angle to prevent vehicle spin. Another task is to maintain the slip angle below a characteristic value to preserve some yaw moment gain. If the slip angle reaches the characteristic value, the gain will be low and the driver may start to notice that he or she is losing control of the vehicle and panic. Therefore, a YMC must start to control the vehicle before this characteristic slip angle value is reached [1].

This study develops BYMC and SYMC based on sliding mode ABS wheel slip control and PID yaw motion control. The control concept of these systems determines by what amount the slip at each tyre is changed to generate the required change in the yaw moment. Previous studies on yaw rate feedback use the desired yaw rate as the reference value [3,13].

The control strategy of a BYMC can be embodied through the slip calculation of the inner rear wheel, because it has the greatest effect on vehicle direction [2]. The optimal slip of the inner rear wheel is calculated using a PID control method. It is transmitted to the wheel slip controller (ABS) to control the braking force (Fig. 3).

The basic control principle of a SYMC is similar to that of a BYMC. The ABS reduces stopping distance and keeps longitudinal stability. The rear wheel steering angle, δ_r , that minimizes the yaw rate error between the desired and measured yaw rates is also calculated using a PID controller [5]. Controllers also determine the direction (CW/CCW) in which the yaw moment should be applied, depending on whether the difference between the actual and refer-

ence yaw rate is positive or negative. Thus the SYMC is a kind of four-wheel steering system.

The control parameter, χ , which is desired slip, in case of BYMC or rear wheel steering angle, in case of SYMC is

$$\chi(k) = \chi(k-1) + (K_p + K_i + K_d)e_\gamma(k) - (K_p + 2K_d)e_\gamma(k-1) + K_d e_\gamma(k-2) \quad (22)$$

where e_γ is the yaw rate error ($-\dot{\gamma}e_\gamma = \dot{\gamma}_{ref}$) and K_p , K_i and K_d are the proportional, integral, and derivative gains, respectively.

4. Simulation results

The developed BYMC and SYMC are evaluated under various maneuvering conditions. The performances of these systems are analyzed and compared to a vehicle equipped with an ABS.

4.1. Wheel slip controller and yaw motion controller evaluation

The straight and curved maneuver is intended to characterize the basic vehicle model and controllers performance. Fig. 4 shows the numerical results on a μ change road, where the target slip, λ_d , for the front and rear wheels is 0.2 regardless of the road condition. The steering input is represented in top left plot of Fig. 4 and full brake pressure (30 bar) is applied at an initial speed of 30 m/s (108 km/h). The vehicle runs on wet asphalt road and passes through snow paved road during 1.5–3.5 s. It is assumed that the friction coefficient, μ , can be estimated approximately.

As shown in top right plot of Fig. 4, slips of front wheels keep 0.2 regardless of road condition and steering wheel input. It depicts the slip follows the target slip value very well and the ABS wheel slip controller is robust. Bottom plots show the reference yaw rate, and the yaw rate of ABS, BYMC and SYMC vehicle. ABS vehicle shows large yaw rate but BYMC and SYMC controller induce the vehicle to follow the reference yaw rate. These results show that although the road condition and steering input are changed, the ABS, BYMC and SYMC controllers keep the desired values, which verifies the robustness of the controllers.

4.2. Effect of road conditions on the yaw motion controller

Figs. 5–10 show the steering input and vehicle response on dry asphalt, wet asphalt, and snow-packed roads. In these simulations, full braking pressure is applied at an initial speed of 30 m/s (108 km/h). Immediately after the braking input is applied, the

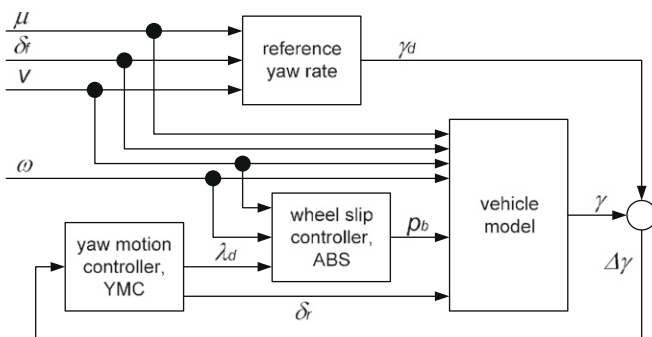


Fig. 3. A schematic of BYMC and SYMC system.

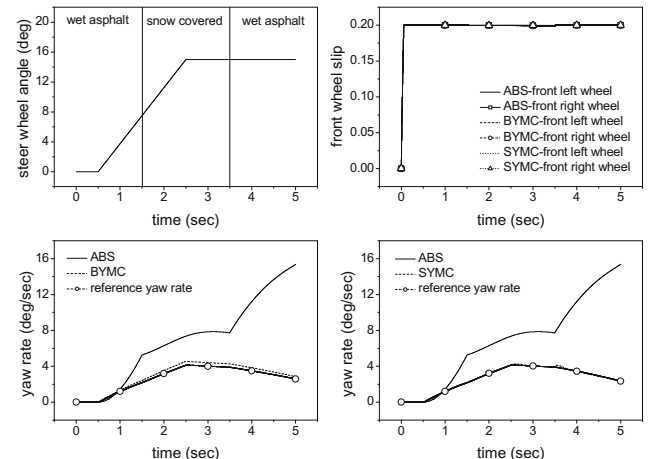


Fig. 4. ABS, BYMC and SYMC vehicle responses on μ change road.

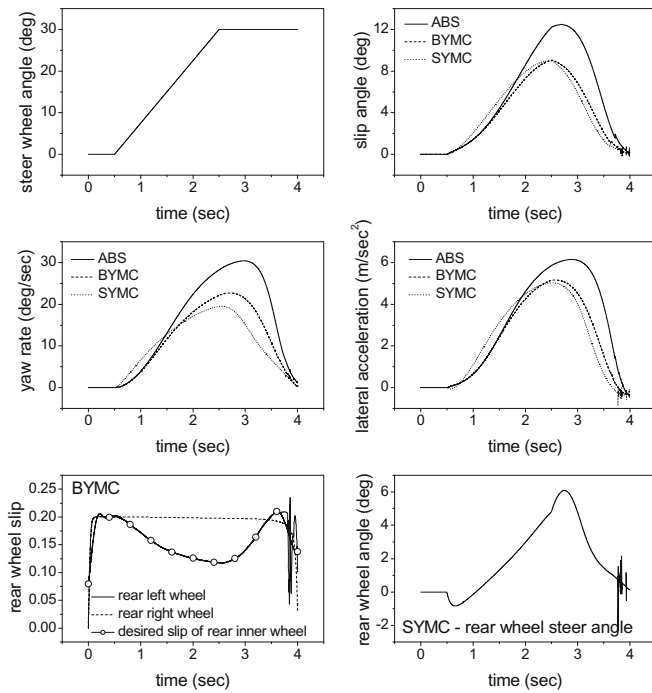


Fig. 5. ABS, BYMC and SYMC vehicle responses on dry asphalt.

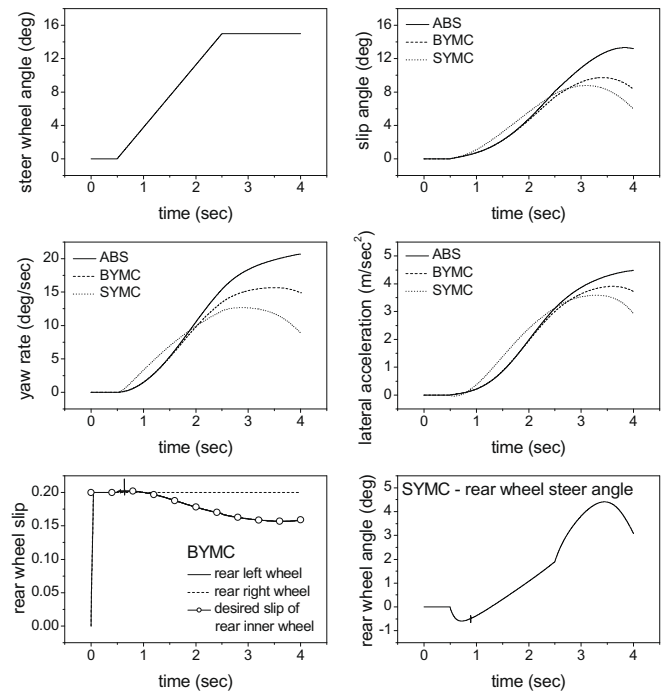


Fig. 7. ABS, BYMC and SYMC vehicle responses on wet asphalt.

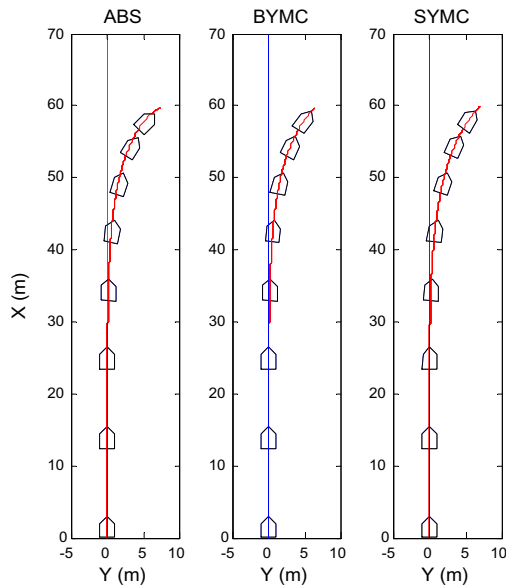


Fig. 6. ABS, BYMC and SYMC vehicle trajectories on dry asphalt.

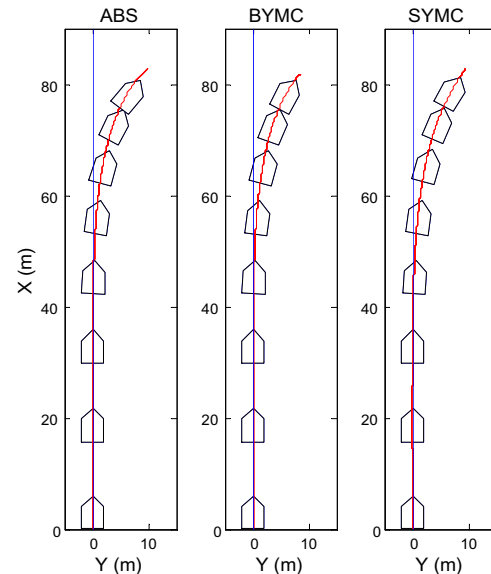


Fig. 8. ABS, BYMC and SYMC vehicle trajectories on wet asphalt.

ABS is engaged to prevent wheel lock. After 0.5 s, the driver starts to turn the steering wheel.

Fig. 5 shows the steering input and vehicle response on dry asphalt. When the BYMC and SYMC are used, the maximum slip angle is reduced by 25%, improving vehicle controllability. Faster increase in the yaw rate and lateral acceleration caused by the SYMC indicates that the vehicle response is also enhanced.

The bottom left plot in Fig. 5 shows the slip of the rear wheels when the BYMC is used, and bottom right plot illustrates the steering angle of the rear wheels when the SYMC is activated. When the BYMC is used, it controls the desired slip of the rear inner wheel, which is the right rear wheel for this driving condition. The ABS modifies the brake pressure of the rear inner wheel to follow the

desired slip; satisfactory results are obtained. Due to the low vehicle velocity, noise occurs after about 3.8 s.

When the SYMC is used, the steering angle of the rear wheels is initially opposite to that of the front wheels, but the direction is changed as the braking maneuver proceeded. The front steering angle is maintained at 5° after 2.5 s and the rear steering angle is reduced to zero because of the vehicle speed reduction. This is different from the classical control strategy of a four-wheel steering vehicle, where the rear wheel steering angle is set opposite to the front wheel steering angle at low speeds and to the same direction as the front wheel steering angle at high speeds [6,14].

The vehicle trajectories are shown in Fig. 6. Although it is difficult to differentiate among the three trajectories, the figure shows

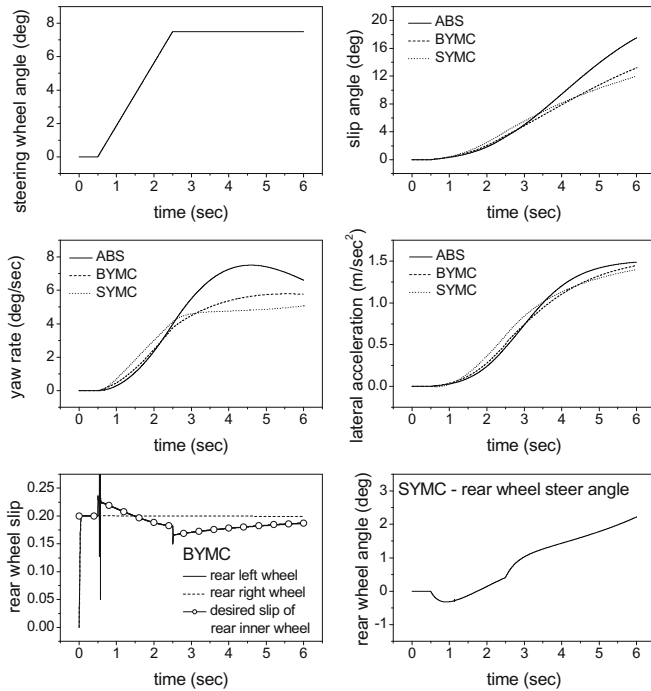


Fig. 9. ABS, BYMC and SYMC vehicle responses on snow paved road.

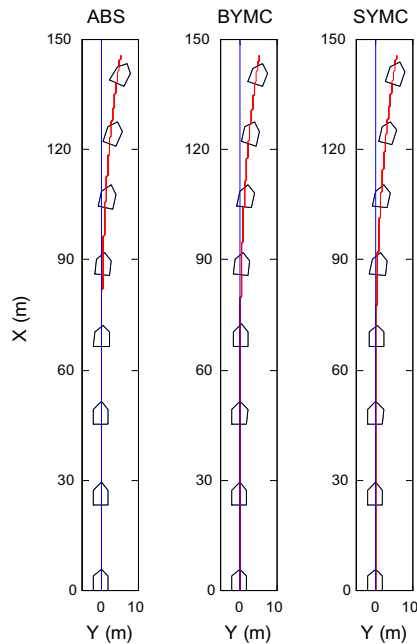


Fig. 10. ABS, BYMC and SYMC vehicle trajectories on snow paved road.

the ABS vehicle travels in a different direction, suggesting that oversteering occurs. According to Wong [15], the turning radius decreases when an oversteered vehicle is decelerated with the steering wheel fixed. The slip angle of the ABS vehicle is much higher, which also indicates that oversteering occurs. With the hard braking, the center of gravity moves to the front of the vehicle, which reduces the braking force applied at the rear wheels. If the rear wheels have an insufficient friction force, they slide outward, so that the vehicle turns into the corner and oversteers. Small changes in the dynamic load transfer, camber changes due to the suspension, trivial changes in the road conditions, or minor

steering or braking inputs from the driver will affect the magnitude and direction of the steering force at the tyres and influence the cornering ability of the vehicle [16].

Fig. 7 shows the response of the vehicle on wet asphalt. The BYMC and SYMC reduce the slip angle, yaw rate, and lateral acceleration. Fig. 8 also demonstrates that the ABS vehicle has the greatest amount of oversteering.

Fig. 9 shows the performances of the ABS, BYMC, and SYMC vehicles on a snow-packed road. Although the steering input is less than that applied in the previous two simulations, the slip angle is the greatest of the simulations and it increased, indicating that the vehicle deceleration is the smallest and the controllability is the worst on the snow-packed road. This driving condition also causes the BYMC and SYMC to reduce the slip angle by 33% and 46%, respectively, at 6 s, improving the lateral characteristics, such as the yaw rate and lateral acceleration. The trajectories of the vehicles are shown in Fig. 10. Oversteering takes place, regardless of the vehicle equipment. The high vehicle velocity and low friction restrict the performance of the yaw motion controllers. However, the ABS vehicle has the largest amount of oversteering because it also had the largest slip angle.

The three simulation results demonstrate that the SYMC vehicle performs better than the BYMC vehicle because SYMC reduces the slip angle. Due to SYMC is a four-wheel steering system that controls the braking pressure and steering angle of the rear wheels simultaneously.

4.3. Sinusoidal input and vehicle response

The response of the vehicles when a sinusoidal steering input is applied is illustrated in Fig. 11. The vehicle runs on wet asphalt with an initial velocity of 30 m/s. The ABS vehicle has the largest slip angle and, as a result, the vehicle loses its lateral controllability. This indicates that the vehicle can not generate enough lateral force at its tyres to change direction. The yaw rate and lateral acceleration responses demonstrate that the steering input is reflected in the vehicle movement very well when the BYMS or SYMC is used. Fennel and Ding [1] reported similar results for a vehicle

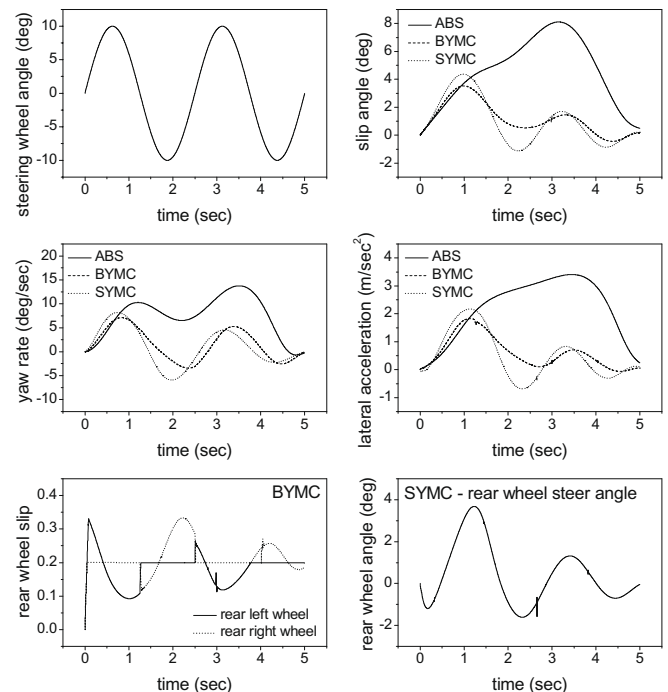


Fig. 11. Sinusoidal input and vehicle responses.

with an ESP, which is similar to a BYMC. They explained that the ABS vehicle has a large slip angle that reduces the coefficient of friction between the tyres and the road.

When a sinusoidal input is applied, the steering control alternates between the left and right rear wheels. The BYMC controller calculates the desired slip of the rear inner wheel, while the ABS controls the brake pressure according to the desired slip. As shown in the bottom left plot, if the left wheel is on the inside of the turn, its slip changes from 0.2 to the desired value, while the slip of the right wheel became 0.2 to reduce the stopping distance.

4.4. Split- μ road and vehicle response

Van Zanten [2] explained that split μ braking presents a special situation for an ESP since the steering angle cannot be interpreted as a cornering desire. Typical commercial ABS systems use an open loop control of the asymmetric braking force gradient on the front tyres and select a low level of control on the rear tyres to maintain control of the vehicle during deceleration. An ESP uses closed loop control of the asymmetric braking forces on the front and rear axles.

A BYMC and SYMC also use closed loop control to allow vehicle to travel straight on a split μ road. When a braking force is generated at the tyres, a yaw motion will begin, due to the friction difference between the left and right wheels. The BYMC and SYMC estimate the yaw rate and compare it with the steering input to determine whether the vehicle is on a split μ road.

Fig. 12 shows the results of full braking on a split μ road (right: dry asphalt; left: wet asphalt) with an initial speed of 30 m/s. The steering input remains zero. When the BYMC or SYMC is applied, the yaw rate, lateral acceleration, and slip angle are small and remain near zero, implying that the vehicle continues forward or changes its direction very slowly. A sudden variation in the yaw motion and lateral acceleration occurs at 1.2 s when the ABS is used, suggesting that the vehicle travels over the centerline so that it is completely on the dry asphalt. The BYMC and SYMC change the rear wheel slip at 2.5 s and the steering angle at 2.2 s, also suggesting that the vehicle travels over the centerline.

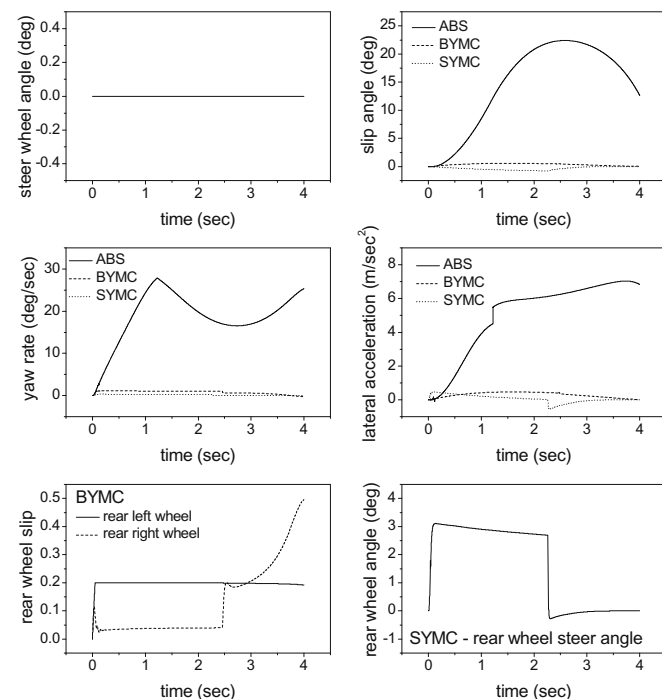


Fig. 12. Vehicle responses on split μ road.

Fig. 13 shows the trajectories of the vehicles. The ABS vehicle shows the largest deviation from a straight line, while the BYMC and SYMC vehicles have only small deviations. These results demonstrate that the BYMC and SYMC enhance the lateral stability of the vehicle and its safety on a split- μ road.

4.5. Lane-change maneuver

The performances of the ABS, BYMC, and SYMC vehicles are verified with a simulated lane-change maneuver. The vehicles are assumed to run on a straight wet asphalt road with an initial velocity of 30 m/s, and braking and steering inputs are applied to avoid a collision.

Fig. 14 shows the desired lateral displacement. A driver model is required to track the desired path. In this paper, the steering angle is assumed to be a function of the estimated lateral offset of the vehicle center of gravity from the desired path (ε) at the look-ahead distance (L), and the yaw angle (γ) of the centre of gravity. This assumption can be represented mathematically as

$$\tau_s \dot{\delta}(t) + \delta(t) = \frac{a_2 V}{(a_1 + L)} \varepsilon(t) + a_3 \dot{\gamma}(t) \quad (23)$$

where V is the vehicle velocity, and a_1 , a_2 , and a_3 are constants. Fig. 15 shows the response of the vehicles. The steering angle decreases for the vehicles equipped with the BYMC or SYMC, suggesting that they are easier to control. The variation of the slip angle and yaw rate are also reduced. Therefore, both the controllability and stability are improved by the BYMC and SYMC.

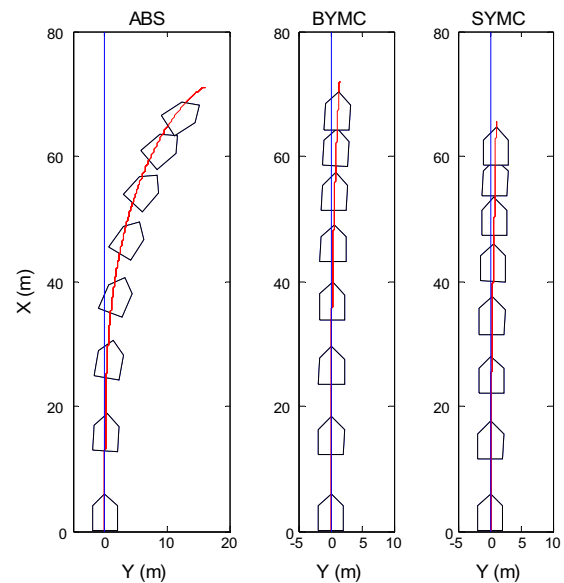


Fig. 13. Vehicle trajectories on split μ road.

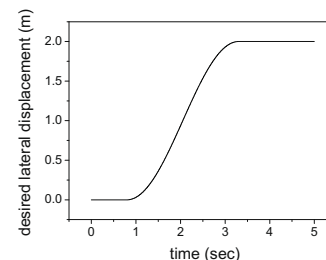


Fig. 14. Desired lateral displacement.

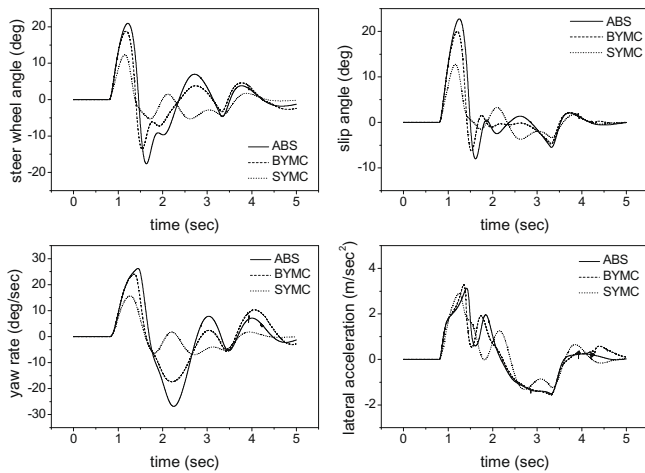


Fig. 15. Vehicle responses during lane-maneuver.

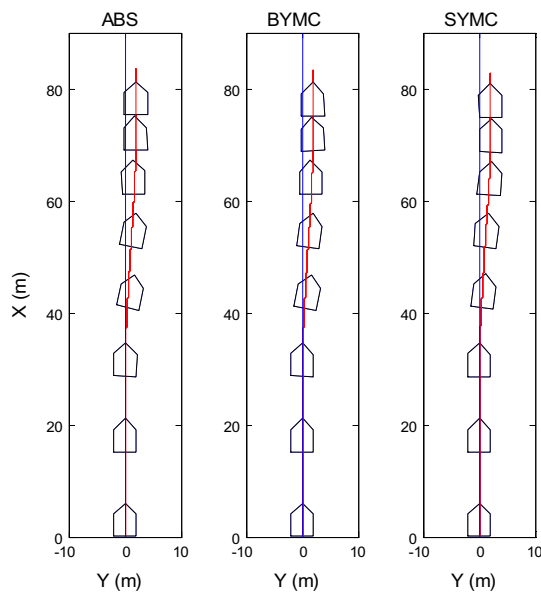


Fig. 16. Vehicle trajectories during lane-change maneuver.

The vehicle trajectories are shown in Fig. 16. The vehicles perform the lane-change maneuver and follow the desired lateral displacement almost perfectly, regardless of whether they are equipped with a yaw motion controller. These results indicate that the driver model can sufficiently control the vehicle to follow the desired path.

5. Conclusions

Two types of vehicle lateral stability control systems are developed in this paper. The first is a braking yaw motion control system that controls the braking pressure of the rear inner wheel; the other is a steering yaw motion control system that controls the steering angle of the rear wheels. A 15 degree-of-freedom nonlinear vehicle model and a simplified steering system model are used

to design the controllers. A sliding mode ABS controller is also developed.

The conclusions from this study are as follows:

- (1) When the vehicle is subjected to a braking and cornering maneuver, the BYMC and SYMC improve its lateral stability and controllability, regardless of the road conditions, because they allow the yaw rate of the vehicle to track the reference yaw rate, reducing the slip angle.
- (2) When full braking pressure and a sinusoidal steering input are applied, both the BYMC and SYMC vehicles have reduced slip angles. The yaw rate and lateral acceleration follow the steering input, indicating that the dynamic response of the vehicle improved.
- (3) When full braking input and no steering input are applied to a vehicle on a split μ road, the vehicle travels to the side of the road with high friction. However, the BYMC and SYMC reduce the deviation, allowing the vehicle to travel forward. The ABS vehicle shows the greatest deviation from the desired path because it is difficult for this system to control the lateral dynamics.
- (4) The driver model tracks the desired vehicle path very well, regardless of whether a yaw motion controller is used. For the lane-change maneuver, the BYMC and SYMC vehicles requires smaller steering inputs. They also have reduced slip angles and yaw rates.
- (5) The SYMC performs better than the BYMC by creating smaller slip angles because the SYMC is basically a four-wheel steering system that controls the braking pressure and steering angle of the rear wheels simultaneously.

References

- [1] Fennel H, Ding EL. A model-based failsafe system for the continental TEVES electronic-stability-program (ESP). SAE2000-01-1635; 2000.
- [2] Van Zanten AT. Bosch ESP systems: 5 years of experience. SAE2000-01-1633; 2000.
- [3] Esmailzadeh E, Goodarzi A, Vossoughi GR. Optimal yaw moment control law for improved vehicle handling. *Mechatronics* 2003;13:659–75.
- [4] Nikzad SV, Naraghi M. Optimizing vehicle response in a combined ride and handling full car model by optimal control strategies. SAE 2001-01-1581; 2001.
- [5] Song J, Boo K. Performance evaluation of traction control systems using a vehicle dynamic model. *Proc Inst Mech Eng Part D* 2004;218(7):685–96.
- [6] Siahkalroudi VN, Naraghi M. Model reference tracking control of a 4WS vehicle using single and dual steering strategies. SAE 2002-01-1590; 2002.
- [7] Song J. Performance evaluation of a hybrid electric brake system with a sliding mode controller. *Mechatronics* 2005;15:339–58.
- [8] Song J, Boo K, Kim HS, Lee J, Hong S. Model development and control methodology of a new electric power steering system. *Proc Inst Mech Eng Part D* 2004;218(9):967–76.
- [9] Gillespie TD. *Fundamentals of vehicle dynamics*. Society of Automotive Engineers; 1992.
- [10] Song J, Kim HS, Kim B. Vehicle longitudinal and lateral stability enhancement using TCS and yaw motion controller. *Int J Autom Technol* 2007;8(1):49–57.
- [11] Kiencke U, Nielsen L. *Automotive control systems*. Society of Automotive Engineers; 2000.
- [12] Park EJ, Stoikov D, da Luz L F, Suleman A. A performance evaluation of an automotive magnetorheological brake design with a sliding mode controller. *Mechatronics* 2006;16(7):405–16.
- [13] Bang MS, Lee SH, Han CS, Maciucă DB, Hedrick JK. Performance Enhancement of a sliding mode wheel slip controller by the yaw motion control. *Proc Inst Mech Eng Part D* 2001;215(4):455–68.
- [14] Sano S, Furukawa Y. Four wheel steering system with rear wheel steering angle controlled as a function of steering wheel angle. SAE 860625; 1986.
- [15] Wong JY. *Theory of ground vehicles*. John Wiley and Sons; 2001.
- [16] Mohan SK, Williams RC. A survey of 4WD traction control systems and strategies. SAE 952644; 1995.